THE JOURNAL OF BIOLOGICAL CHEMISTRY VOL. 284, NO. 43, pp. 29320–29325, October 23, 2009

Extracellular Chloride Regulates the Epithelial Sodium Channel*

Received for publication, July 20, 2009, and in revised form, August 26, 2009 Published, JBC Papers in Press, August 27, 2009, DOI 10.1074/jbc.M109.046771

Daniel M. Collier and Peter M. Snyder[1]

From the Departments of Internal Medicine and Molecular Physiology and Biophysics, Roy J. and Lucille A. Carver College of Medicine, University of Iowa, Iowa City, Iowa 52242

The extracellular domain of the epithelial sodium channel ENaC is exposed to a wide range of Cl^- concentrations in the kidney and in other epithelia. We tested whether Cl^- alters ENaC activity. In *Xenopus* oocytes expressing human ENaC, replacement of Cl^- with SO_4^{2-}, $H_2PO_4^-$, or SCN^- produced a large increase in ENaC current, indicating that extracellular Cl^- inhibits ENaC. Extracellular Cl^- also inhibited ENaC in Na^+-transporting epithelia. The anion selectivity sequence was $SCN^- < SO_4^{2-} < H_2PO_4^- < F^- < I^- < Cl^- < Br^-$. Crystallization of ASIC1a revealed a Cl^- binding site in the extracellular domain. We found that mutation of corresponding residues in ENaC (α_{H418A} and β_{R388A}) disrupted the response to Cl^-, suggesting that Cl^- might regulate ENaC through an analogous binding site. Maneuvers that lock ENaC in an open state (a DEG mutation and trypsin) abolished ENaC regulation by Cl^-. The response to Cl^- was also modulated by changes in extracellular pH; acidic pH increased and alkaline pH reduced ENaC inhibition by Cl^-. Cl^- regulated ENaC activity in part through enhanced Na^+ self-inhibition, a process by which extracellular Na^+ inhibits ENaC. Together, the data indicate that extracellular Cl^- regulates ENaC activity, providing a potential mechanism by which changes in extracellular Cl^- might modulate epithelial Na^+ absorption.

The epithelial Na^+ channel ENaC[2] is a heterotrimer of homologous α, β, and γ subunits (1, 2). ENaC functions as a pathway for Na^+ absorption across epithelial cells in the kidney collecting duct, lung, distal colon, and sweat duct (reviewed in Refs. 3 and 4). Na^+ transport is critical for the maintenance of Na^+ homeostasis and for the control of the composition and quantity of the fluid on the apical membrane of these epithelia. ENaC mutations and defects in its regulation cause inherited forms of hypertension and hypotension (5) and may contribute to the pathogenesis of lung disease in cystic fibrosis (6).

ENaC is a member of the DEG/ENaC family of ion channels. A common structural feature of these channels is a large extracellular domain that plays a critical role in channel gating. For example, in ASICs, the extracellular domain functions as a receptor for protons, which transiently activate the channel by titrating residues that form an acidic pocket (7). FaNaCh is a ligand-gated family member in *Helix aspersa*, activated by the peptide FMRFamide (8). In *Caenorhabditis elegans* MEC family members, the extracellular domain is thought to respond to mechanical signals (9).

ENaC differs from other family members because it is constitutively active in the absence of a ligand/stimulus. However, a convergence of data indicate that ENaC gating is modulated by a variety of molecules that bind to or modify its extracellular domains, including proteases (10–12), Na^+ (13–15), protons (16), and the divalent cations Zn^{2+} and Ni^{2+} (17, 18). These findings suggest that the ENaC extracellular domain might regulate epithelial Na^+ transport by sensing and integrating diverse signals in the extracellular environment.

In the current study, we tested the hypothesis that ENaC activity is regulated by changes in the extracellular Cl^- concentration. Several observations suggested that Cl^- might be a strong candidate to regulate the channel. First, transport of Na^+ and Cl^- are often coupled to maintain electroneutrality. Second, ENaC is exposed to large changes in extracellular Cl^- concentration. For example, in the kidney collecting duct, the urine Cl^- concentration varies widely (19). As the predominant anion, its concentration parallels that of Na^+ in most clinical states. However, under conditions of metabolic alkalosis and metabolic acidosis, the Na^+ and Cl^- concentrations can become dissociated as a result of increased urinary bicarbonate (alkalosis) or ammonium (acidosis) (19). Thus, ENaC is well positioned to respond to changes in Cl^- concentration. Third, crystallization of ASIC1a revealed a binding site for a Cl^- ion at the base of the thumb domain (7). The Cl^- is coordinated by Arg-310 and Glu-314 from one subunit and Lys-212 from an adjacent subunit. Although the functional role of Cl^- binding to ASIC1a is unknown, it supports the hypothesis that extracellular Cl^- might regulate the activity of DEG/ENaC ion channels.

EXPERIMENTAL PROCEDURES

DNA Constructs—cDNAs for human αENaC, βENaC, and γENaC in pMT3 were cloned as described previously (2, 20). The mutations α_{H418A}, β_{R388A}, γ_{H396A}, and γ_{H233R} were generated by site-directed mutagenesis (QuikChange; Stratagene) and sequenced in the University of Iowa DNA Core.

Expression and Whole-cell Electrophysiology in Xenopus Oocytes—Oocytes were harvested from albino *Xenopus laevis* females and manually defolliculated following a 1-h treatment with 0.75 mg/ml type IV collagenase (Sigma) in Ca^{2+}-free ND-96 (96 mM NaCl, 2 mM KCl, 1 mM $MgCl_2$, 5 mM HEPES, pH

* This work was supported, in whole or in part, by National Institutes of Health Grants HL058812 and HL72256 (to P. M. S.).

[1] To whom correspondence should be addressed: 371 EMRB, University of Iowa, IA City, IA 52242. E-mail: peter-snyder@uiowa.edu.

[2] The abbreviations used are: ENaC, epithelial sodium channel; ASIC, acid-sensitive ionic channel subunit; MTSET, methanethiosulfonate ethyltrimethylammonium.

adjusted to 7.4 with NaOH). Following nuclear injection of cDNAs encoding αENaC, βENaC, and γENaC (0.02 μg/μl each), cells were incubated at 18 °C in modified Barth's saline (88 mM NaCl, 1 mM KCl, 0.33 mM $Ca(NO_3)_2$, 0.41 mM $CaCl_2$, 0.82 mM $MgSO_4$, 2.4 mM $NaHCO_3$, 10 mM HEPES, 50 μg/ml gentamycin sulfate, 10 μg/ml sodium penicillin, 10 μg/ml streptomycin sulfate, pH adjusted to 7.4 with NaOH) for 20–24 h prior to study. Oocytes were voltage-clamped (two-electrode voltage clamp), and currents were amplified with an oocyte clamp OC-725C (Warner Instruments), digitized with a MacLab/200 interface (ADInstruments), and recorded and analyzed with the Chart software (ADInstruments). The bathing solution was grounded with 3 M KCl-agar bridges to prevent junction potentials during changes in Cl^- concentration. Unless otherwise noted, recordings were done at −60 mV in a 116 mM NaCl solution (116 mM NaCl, 2 mM KCl, 0.4 mM $CaCl_2$, 1 mM $MgCl_2$, 5 mM HEPES, pH adjusted to 7.4 with NaOH). Low Na^+ solutions (1 mM NaCl, 115 mM *N*-methyl-D-glucamine Cl or SO_4, pH adjusted with HCl or H_2SO_4) were used as indicated in the legend for Fig. 5. Low chloride solutions were prepared by replacing the anion of the sodium salt with I^-, Br^-, F^-, SCN^-, $H_2PO_4^-$, or SO_4^{2-} and D-mannitol (to balance osmolarity). Amiloride-sensitive current was determined by adding 10 μM amiloride to the bathing solution. The pH and chloride-induced changes in amiloride-sensitive current were calculated as the -fold increase/decrease relative to the baseline current in pH 7.4, 116 NaCl solution, just prior to each test solution application. This was done to reduce the effect of time-dependent current rundown. The resulting data were plotted and fit to the Hill equation using the IGOR Pro software (WaveMetrics Inc.). Na^+ self-inhibition was measured by rapidly changing the bathing solution from low sodium (1 mM) to high sodium (116 mM) and quantitated as (peak current −steady state current)/peak current.

Expression and Whole-cell Electrophysiology in H441 and Primary Airway Epithelia—H441 cells (American Type Culture Collection) were grown on 0.6-cm^2 permeable filter supports (Millipore) in RPMI with 8.5% fetal calf serum, 20 mM L-glutamine, 5 μg/ml insulin, 5 μg/ml transferrin, 5 ng/ml selenium, 100 nm dexamethasone, 100 units/ml penicillin, and 100 mg/ml streptomycin at 37 °C for 5 days. Primary human airway epithelia were isolated from the trachea and bronchi of donor lungs and grown at the air-liquid interface of collagen-coated permeable filter supports, as described previously (21). Aprotinin (26 μg/ml) was present in the apical solution for 2 h prior to study. Short circuit Na^+ current was measured in modified Ussing chambers (Warner Instrument Corp.) using an EC-825 epithelial voltage clamp amplifier (Warner Instrument Corp.). Currents were digitized with a PowerLab interface (ADInstruments) and recorded and analyzed with the Chart software (ADInstruments). The apical and basolateral surfaces were bathed in 116 mM NaCl, 2 mM KCl, 0.4 mM $CaCl_2$, 1 mM $MgCl_2$, 5 mM HEPES (pH adjusted to 7.4 with NaOH) or with 58 mM Na_2SO_4, 58 mM D-mannitol, 2 mM KCl, 0.4 mM $CaCl_2$, 1 mM $MgCl_2$, 5 mM HEPES (pH adjusted to 7.4 with NaOH) at 37 °C. The amiloride-sensitive short circuit current was determined as the difference in current with and without amiloride (10 μM) in the apical bathing solution.

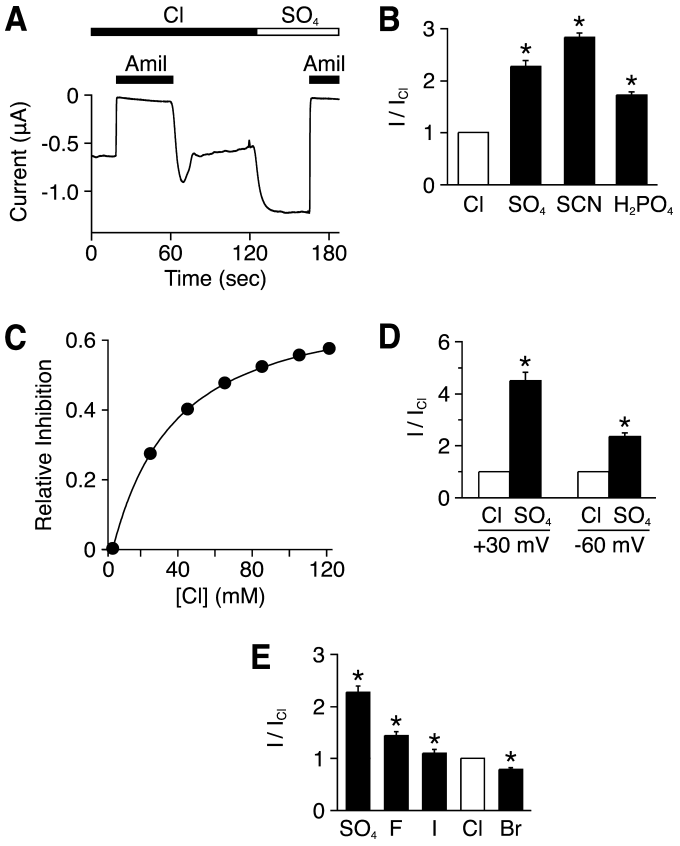

FIGURE 1. **Extracellular anions modulate ENaC activity.** *A*, representative trace of current *versus* time from a *Xenopus* oocyte expressing human αβγ ENaC clamped at −60 mV. The bathing solution contained Cl^- or SO_4^{2-}, as indicated. Amiloride (*Amil*, 10 μM) was present in the bathing solution, as indicated by the *black bars*. *B*, amiloride-sensitive current with the indicated anion in the bathing solution (relative to Cl^-) (mean ± S.E. (*error bars*), n = 5–23, *, $p < 0.01$). *C*, fraction of amiloride-sensitive current inhibited *versus* extracellular Cl^- concentration (total anion concentration held constant with SO_4^{2-}) (mean ± S.E., $n = 9$, error bars are hidden by the data points). *D*, amiloride-sensitive current with Cl^- or SO_4^{2-} in the bathing solution (relative to Cl^-) at a holding potential of −60 mV (inward current) or +30 mV (outward current) (mean ± S.E. (*error bars*), n = 10–11, *, $p < 0.01$. *E*, amiloride-sensitive current when Cl^- in the bathing solution was replaced with the indicated anion (relative to Cl^-) (mean ± S.E. (*error bars*), n = 9–23, *, $p < 0.01$).

RESULTS

Extracellular Anions Modulate ENaC Current—To determine whether extracellular Cl^- modulates ENaC current, we replaced Cl^- with other anions and recorded ENaC currents in *Xenopus* oocytes expressing human αENaC, βENaC, and γENaC. When Cl^- was replaced by SO_4^{2-}, amiloride-sensitive ENaC current increased by 2.4-fold (Fig. 1, *A* and *B*). This increase was rapid and reversible (see Fig. 4*B*). Replacement of Cl^- with $H_2PO_4^-$ and SCN^- also increased ENaC current (Fig. 1*B*). As a control, Cl^- replacement did not significantly alter current in oocytes not expressing ENaC (not shown). We also excluded the possibility that SO_4^{2-} and $H_2PO_4^-$ altered ENaC current by lowering Ca^{2+} activity in the bathing solution; the effect of Cl^- replacement was not reduced when Ca^{2+} activity was held constant (not shown).

Fig. 1*C* shows a dose-response relationship for Cl^-. As extracellular Cl^- increased (replacing SO_4^{2-}), there was a dose-dependent decrease in ENaC current. The maximal fraction of ENaC current inhibited by Cl^- was 0.73, and half-maximal

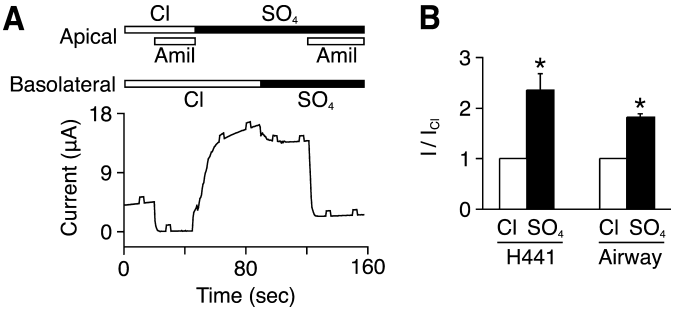

FIGURE 2. **Extracellular Cl^- modulates endogenous ENaC activity in epithelia.** *A*, representative short circuit current trace in H441 cells. The apical and basolateral bathing solutions contained Cl^- or SO_4^{2-}, as indicated. Amiloride (*Amil*, 10 μM) was added to the apical bathing solution, as indicated by the *gray bars*. 0.5-mV pulses were applied every 15 s to monitor resistance. *B*, amiloride-sensitive current with Cl^- or SO_4^{2-} in the bathing solution (relative to Cl^-) in H441 and primary airway epithelial cells (mean ± S.E. (*error bars*), $n = 5–6$, *, $p < 0.01$).

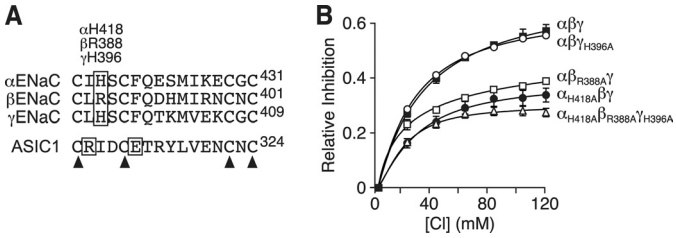

FIGURE 3. **Identification of residues that participate in Cl^- regulation of ENaC.** *A*, sequence alignment of human αENaC, βENaC, and γENaC and chicken ASIC1a. *Boxes* indicate residues that bind Cl^- in ASIC1a and potential equivalent residue in ENaC. *Arrowheads* indicate conserved cysteine residues. *B*, fraction of amiloride-sensitive current inhibited by Cl^- (replacing SO_4^{2-}) in oocytes expressing the indicated ENaC subunits (mean ± S.E. (*error bars*), $n = 6–9$). Some of the error bars are hidden by the data points.

inhibition occurred at a Cl^- concentration of 29.5 ± 0.25 mM. The data indicate that Cl^- inhibits ENaC current at concentrations found in the kidney collecting duct and other epithelia (19).

We considered the possibility that removal of extracellular Cl^- could alter ENaC current by reducing the concentration of intracellular Cl^- (22). To exclude this possibility, we voltage-clamped cells at +30 mV to prevent movement of Cl^- out of the cell. Under these conditions, replacement of Cl^- with SO_4^{2-} still increased amiloride-sensitive current (Fig. 1*D*). This result indicates that changes in extracellular Cl^- are sufficient to alter ENaC current.

We asked whether other anions could substitute for Cl^-. When compared with SO_4^{2-}, I^-, Br^-, and F^- each decreased ENaC current. F^- and I^- decreased current to a smaller extent than Cl^-, and Br^- produced a larger decrease in current (Fig. 1*E*). Thus, the anion selectivity sequence for ENaC inhibition is $SCN^- < SO_4^{2-} < H_2PO_4^- < F^- < I^- < Cl^- < Br^-$.

Cl^- Inhibits ENaC in Epithelia—To test the effect of extracellular chloride on native ENaC in epithelial cells, we measured short circuit current. In a human lung carcinoma cell line (H441), we measured amiloride-sensitive current when the apical and basolateral membranes were bathed in NaCl (Fig. 2*A*). When Cl^- was replaced with SO_4^{2-} on the apical and basolateral membranes (to eliminate a Cl^- gradient), there was an increase in amiloride-sensitive current (Fig. 2*A* and quantitated in Fig. 2*B*). Results were similar in primary cultures of human airway epithelia (Fig. 2*B*). Thus, Cl^- regulates ENaC both in *Xenopus* oocytes and in Na^+-transporting epithelia.

Identification of Residues That Participate in Cl^- Regulation of ENaC—We hypothesized that Cl^- might regulate ENaC by binding to a site analogous to the Cl^- binding site observed in the crystal structure of ASIC1a (7). To identify candidate residues, we lined up the ASIC1a and ENaC sequences. In general, sequence conservation in the extracellular domains is low. We therefore focused on a portion of the thumb domain where the lineup was facilitated by the presence of four highly conserved cysteine residues (Fig. 3*A*). In ASIC1a, the positively charged side chain of Arg-310 participates in the coordination of Cl^-. In βENaC, an arginine is located one position downstream (β-Arg-388). The equivalent residues in αENaC and γENaC are histidine (418 and 396, respectively), which when protonated carry a positive charge that could coordinate Cl^-.

To test their role in Cl^- regulation of ENaC, we mutated each of these residues to alanine. In Fig. 3*B*, we expressed wild-type or mutant (α_{H418A}, β_{R388A}, and γ_{H396A}) ENaC in *Xenopus* oocytes and varied the extracellular Cl^- concentration. When compared with wild-type ENaC, the mutations reduced Cl^--dependent inhibition by more than 50%. We also tested the effect of mutations in individual ENaC subunits. ENaC currents in cells expressing $\alpha_{H418A}\beta\gamma$ ENaC or $\alpha\beta_{R388A}\gamma$ ENaC were also less responsive to Cl^-, whereas Cl^- inhibited $\alpha\beta\gamma_{H396A}$ channels similar to wild-type (Fig. 3*B*). Together, these results suggest that α-His-418 and β-Arg-388 participate in ENaC regulation by Cl^-. Although we cannot exclude a role for γ-His-396, this residue is not required for Cl^- to inhibit ENaC. Because mutation of these residues did not completely abolish the effect of Cl^- on ENaC, it seems likely that additional residues also contribute.

DEG Mutation and Proteolytic Cleavage Abolish Response to Cl^-—Because Cl^- removal or readdition altered ENaC current over a rapid time course (in seconds), it seemed likely that Cl^- affected channel activity rather than changing ENaC trafficking. To more directly test this idea, we used two strategies to prevent changes in ENaC activity. First, we covalently modified a cysteine introduced at the DEG position at the extracellular end of the pore in βENaC (β_{S520C}), a maneuver that locks ENaC in the open state (open probability = 0.96) (23). Fig. 4*A* shows an oocyte expressing $\alpha\beta_{S520C}\gamma$ ENaC before (*black line*) and after (*gray line*) modification with MTSET. To emphasize the Cl^--dependent effect, the traces were normalized to the peak currents and superimposed. Before modification, Cl^- decreased current similar to wild-type ENaC (Fig. 4, *A*, *black line*, and *B*). In contrast, Cl^- had no effect on ENaC current after the introduced cysteine was modified with MTSET (Fig. 4, *A*, *gray line*, and *B*). As a second strategy, we took advantage of the observation that ENaC gating is disrupted by proteolytic cleavage of the extracellular domain, which also increases open probability (12). Treatment of wild-type ENaC with trypsin (2 μg/ml for 3 min) abolished the effect of Cl^- on current (Fig. 4, *C*, *gray line*, and *D*). Together, the data indicate that Cl^- is incapable of inhibiting ENaC channels that are locked in an open conformation or that are proteolytically cleaved and activated by trypsin.

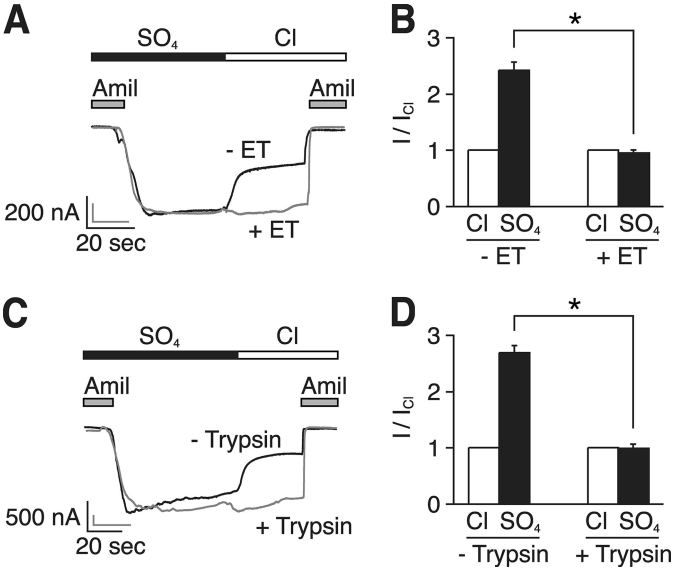

FIGURE 4. **DEG mutation and proteolytic cleavage abolish response to Cl^-.** *A*, representative current traces at a holding potential of −60 mV in the same *Xenopus* oocyte expressing human $\alpha\beta_{S520C}\gamma$ ENaC before (*black trace*) and after (*gray trace*) modification with MTSET (*ET*). The bathing solution contained SO_4^{2-} or Cl^-, as indicated. 10 μM amiloride (*Amil*) was present in the bathing solution, as indicated by the *gray bars*. *B*, amiloride-sensitive current in oocytes expressing $\alpha\beta_{S520C}\gamma$ ENaC with Cl^- or SO_4^{2-} in the bathing solution (relative to Cl^-) before and after treatment of with MTSET (mean ± S.E. (*error bars*), $n = 3$, *, $p < 0.01$). *C*, representative current traces at a holding potential of −60 mV in the same *Xenopus* oocyte expressing human $\alpha\beta\gamma$ ENaC before (*black trace*) and after (*gray trace*) treatment with trypsin (2 μg/ml). *D*, amiloride-sensitive current in oocytes expressing $\alpha\beta\gamma$ ENaC with Cl^- or SO_4^{2-} in the bathing solution (relative to Cl^-) before and after treatment with trypsin (mean ± S.E. (*error bars*), $n = 4$, *, $p < 0.001$).

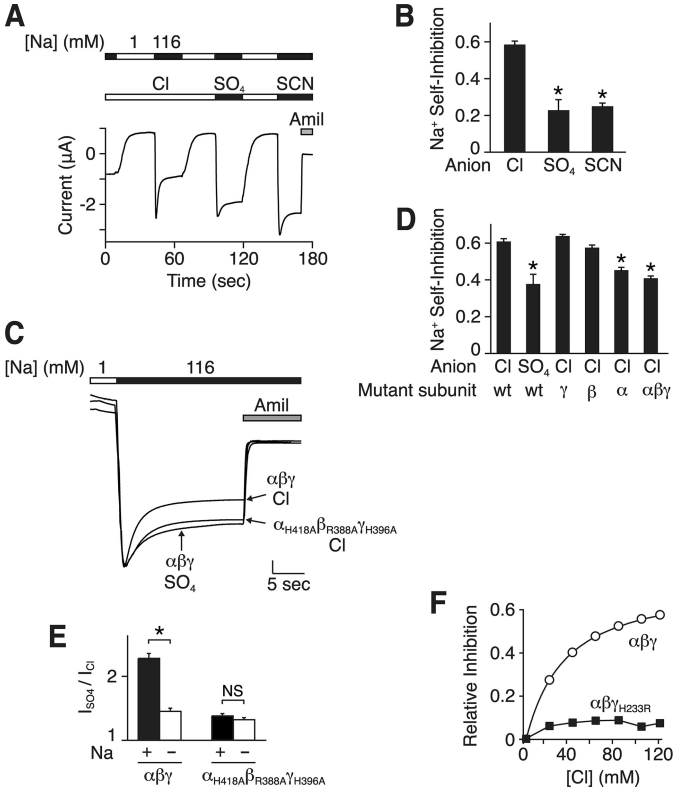

FIGURE 5. **Cl^- alters Na^+ self-inhibition.** *A*, representative current trace showing Na^+ self-inhibition in *Xenopus* oocytes expressing human $\alpha\beta\gamma$ ENaC with Cl^-, SO_4^{2-}, or SCN^- in the bathing solution. The extracellular Na^+ concentration was 1 (*white bars*) or 116 mM (*black bars*), as indicated. 10 μM amiloride (*Amil*) was present in the bathing solution, as indicated by the *gray bar*. *B*, summary data of Na^+ self-inhibition ((peak current − steady-state current)/peak current) with Cl^-, SO_4^{2-}, or SCN^- bathing solutions (mean ± S.E. (*error bars*), $n = 6–7$, *, $p < 0.001$). *C*, representative current traces showing Na^+ self-inhibition in *Xenopus* oocytes expressing wild-type or mutant (α_{H418A}, β_{R388A}, and γ_{H396A}) ENaC in Cl^- or SO_4^{2-} bathing solution, as indicated. The traces are scaled to the peak amiloride-sensitive currents. The *vertical scale bar* is 1.7 ($\alpha\beta\gamma$ Cl^-), 0.6 ($\alpha\beta\gamma$ SO_4^{2-}), and 1.9 μA (α_{H418A}, β_{R388A}, and γ_{H396A} Cl^-). *D*, Na^+ self-inhibition in oocytes expressing $\alpha\beta\gamma$ ENaC, wild type (*wt*), or the indicated mutant subunits (α_{H418A}, β_{R388A}, or γ_{H396A}). Bathing solution contained Cl^- or SO_4^{2-}, as indicated. Data are mean ± S.E. (*error bars*), $n = 4–16$, *, $p < 0.01$ *versus* wild-type in Cl^-. *E*, ratio of amiloride-sensitive current in SO_4^{2-} *versus* Cl^- bathing solution in oocytes expressing wild-type or mutant ENaC and incubated in 116 mM Na^+ (+) or 1 mM Na^+ (−) (mean ± S.E. (*error bars*), $n = 3–14$, *, $p < 0.01$). Holding potential was −60 mV. Inward current was recorded for cells in 116 mM Na^+, and outward current was recorded for cells in 1 mM Na^+. *F*, fraction of amiloride-sensitive current inhibited *versus* extracellular Cl^- concentration for wild-type or mutant ($\alpha\beta\gamma_{H233R}$) ENaC (mean ± S.E., $n = 3–9$, error bars are hidden by the data points).

Cl^- Alters Na^+ Self-inhibition—ENaC is regulated in part by changes in extracellular Na^+ (Na^+ self-inhibition) (13–15). We hypothesized that Cl^- might inhibit ENaC by modulating the effect of Na^+ on ENaC. To test this, we quantitated Na^+ self-inhibition with Cl^- or SO_4^{2-} as the predominant anion in the extracellular bathing solution. In *Xenopus* oocytes expressing ENaC, a rapid increase in extracellular Na^+ (from 1 to 116 mM) produced an inward Na^+ current (downward deflection) that rapidly decreased to a lower steady-state level, as a result of Na^+ self-inhibition (Fig. 5*A*). When Cl^- was the anion, the fraction of amiloride-sensitive current inhibited by Na^+ was 0.58 ± 0.02 (Fig. 5*B*). When Cl^- was replaced by SO_4^{2-} or SCN^-, a smaller fraction of ENaC current was inhibited by Na^+ (0.23 ± 0.06 and 0.25 ± 0.02, respectively) (Fig. 5, *A* and *B*). Mutation of the putative Cl^- binding site in all three subunits (α_{H418A}, β_{R388A}, and γ_{H396A}) reduced Na^+ self-inhibition to a similar extent as Cl^- removal (Fig. 5, *C* and *D*). Na^+ self-inhibition was also reduced by mutation of the α subunit alone but not by mutation of βENaC or γENaC (Fig. 5*D*).

The data suggest that Cl^- inhibits ENaC in part by increasing Na^+ self-inhibition. If correct, then removal of Na^+ from the extracellular solution should disrupt the effect of anion substitution on ENaC current. To test this prediction, we replaced extracellular Na^+ with *N*-methyl-D-glucamine and measured outward amiloride-sensitive current. Under these conditions, substitution of extracellular Cl^- with SO_4^{2-} increased ENaC current much less ($I_{SO_4^{2-}}/I_{Cl^-} = 1.46 \pm 0.06$) than when Na^+ was present in the extracellular solution ($I_{SO_4^{2-}}/I_{Cl^-} = 2.38 \pm 0.12$) (Fig. 5*E*). In contrast, when the putative Cl^- binding sites were mutated, the residual effect of anion substitution was not altered by changes in extracellular Na^+ (Fig. 5*E*).

As a further test of the role of Na^+ self-inhibition in ENaC regulation by Cl^-, we mutated a residue required for Na^+ self-inhibition. Previous work found that mutation of His-239 in the extracellular domain of mouse γENaC abolished Na^+ self-inhibition (15). Mutation of the equivalent residue in human γENaC (His-233) had a similar effect (16). We tested whether this mutation ($\alpha\beta\gamma_{H233R}$) would disrupt the effect of Cl^- on ENaC. In contrast to wild-type ENaC, changes in Cl^- concentration had little effect on the mutant channel (Fig. 5*F*). Together, the data suggest that Cl^- regulates ENaC in part by modulating Na^+ self-inhibition.

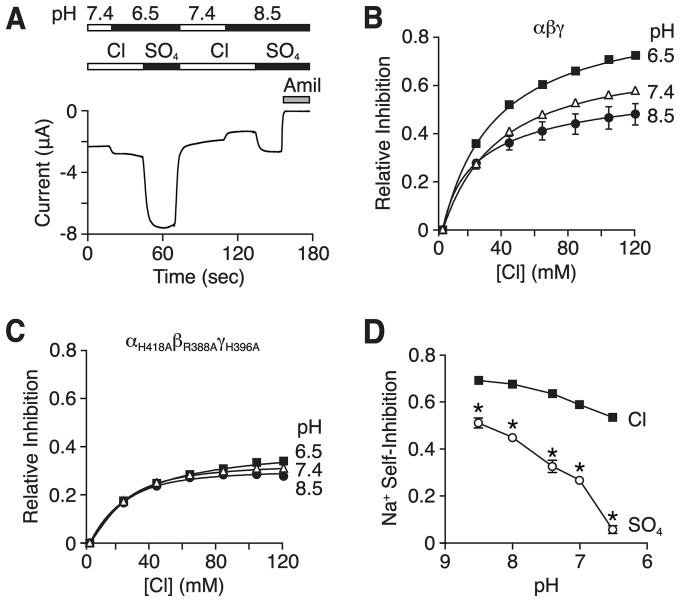

FIGURE 6. **pH modulates the effect of Cl^- on ENaC.** *A*, representative current trace at a holding potential of −60 mV in a *Xenopus* oocyte expressing human $\alpha\beta\gamma$ ENaC. pH of bathing solution was 8.5, 7.4, or 6.5, and it contained Cl^- or SO_4^{2-}, as indicated. 10 μM amiloride (*Amil*) was present in the bathing solution, as indicated by the *gray bar*. *B* and *C*, fraction of amiloride-sensitive current inhibited by Cl^- (replacing SO_4^{2-}) in oocytes expressing wild-type (*B*) or α_{H418A}, β_{R388A}, and γ_{H396A} (*C*) ENaC (mean ± S.E. (*error bars*), $n = 3$–9). *D*, pH dose-response relationship for Na^+ self-inhibition of $\alpha\beta\gamma$ ENaC in Cl^- or SO_4^{2-} bathing solution (mean ± S.E. (*error bars*), $n = 4$–14, *, $p < 0.01$ *versus* Cl^-). In *panels B–D*, some of the error bars are hidden by the data points.

pH Modulates the Effect of Cl^- on ENaC—If the histidines we identified in Fig. 3 are Cl^- binding sites, then we might expect ENaC regulation by Cl^- to be altered by changes in extracellular pH. The imidazole side chain of histidine has a relatively neutral pK_a (6.0), although this value can shift depending on its local environment. At alkaline pH, the side chain is uncharged, but at acidic pH, it is protonated and carries a positive charge, which could enhance Cl^- binding through electrostatic effects. To test this prediction, we varied the pH in the bathing solution and replaced Cl^- with SO_4^{2-}. Fig. 6*A* shows a representative current trace. At pH 6.5, Cl^- removal produced a large increase in amiloride-sensitive current. At pH 8.5, Cl^- removal also increased current, but the increase was smaller than at pH 6.5. Fig. 6*B* shows Cl^- dose-response relationships at pH 6.5, 7.4, and 8.5. When compared with pH 7.4, Cl^- inhibition of ENaC was increased at acidic pH and reduced at alkaline pH. Mutation of the putative Cl^- binding residues (α_{H418A}, β_{R388A}, and γ_{H396A}) abolished the effect of pH on ENaC inhibition by Cl^- (Fig. 6*C*). Thus, ENaC regulation by Cl^- is modulated by changes in extracellular pH.

Because protons increase ENaC inhibition by Cl^-, this effect should tend to reduce ENaC current at acidic pH. However, in previous work, we observed the opposite; acidic pH increased ENaC current (16) (in Fig. 6*A*, compare the current at pH 6.5, 7.4, and 8.5 with Cl^- bathing solution). This resulted from a decrease in Na^+ self-inhibition at acidic pH (16) (Fig. 6*D*, *Cl*). We hypothesized that protons have two opposing effects on Na^+ self-inhibition; one alters Cl^- binding and increases self-inhibition (which decreases current), whereas the other is independent of Cl^- and reduces self-inhibition (which increases current). To eliminate the Cl^--dependent component, we removed Cl^- from the bathing solution and tested the effect of protons on Na^+ self-inhibition. Under these conditions, the inhibitory effect of protons on Na^+ self-inhibition was greatly enhanced; acidic pH decreased Na^+ self-inhibition to a larger extent than when Cl^- was the extracellular anion (Fig. 6*D*). Thus, although protons tend to decrease ENaC current through their effect on Cl^- binding, this is countered by an independent inhibitory effect of protons on Na^+ self-inhibition. The net result is increased ENaC current at acidic pH.

DISCUSSION

Our findings in heterologous cells and in Na^+-transporting epithelia indicate that ENaC is regulated by changes in extracellular Cl^-. As the concentration of extracellular Cl^- increased, we observed a dose-dependent reduction in ENaC Na^+ current.

Cl^- could regulate ENaC directly by binding to the channel or indirectly through interactions with lipids in the plasma membrane. Based on two observations, we favor direct binding of Cl^- to ENaC. First, the crystal structure of ASIC1a (7) identified a Cl^- binding site in its extracellular domain, raising the possibility that an analogous site is present in ENaC. Second, Cl^- inhibition of ENaC was reduced by mutation of residues in αENaC (His-418) or βENaC (Arg-388) that correspond to the ASIC1a Cl^- binding site. Thus, it seems likely that these residues contribute to Cl^- binding in ENaC. However, mutation of these residues did not completely abolish the effect of Cl^- on ENaC current. In ASIC1, Cl^- is coordinated by three residues (7), so it is possible that there is residual Cl^- binding to other ENaC residues. Alternatively, it is possible that Cl^- regulates ENaC in part through binding to a second site or through a mechanism independent of channel binding.

Our data indicate that Cl^- inhibits ENaC through a change in channel activity. Maneuvers that locked the channel in a high open probability state (a DEG mutation and trypsin) abolished the effect of Cl^- on ENaC current. This finding is most consistent with a model in which Cl^- regulates ENaC predominately through a change in channel gating, although we cannot exclude additional effects on ENaC trafficking or single channel conductance. How might this occur? Previous work indicates that ENaC gating is regulated in part by extracellular Na^+, which inhibits the channel (Na^+ self-inhibition) (13–15). We found that Na^+ self-inhibition was reduced in the absence of extracellular Cl^-. This finding supports a model in which Cl^- inhibits ENaC gating by stabilizing the Na^+ self-inhibited state. Perhaps the binding of Na^+ to ENaC is enhanced when the channel is bound to Cl^-. However, changes in Na^+ self-inhibition do not completely explain the effects of Cl^- on ENaC current. For example, upon removal of Na^+ from the extracellular bathing solution, the effect of Cl^- on ENaC was dramatically reduced but not abolished (Fig. 5*E*). Moreover, mutation of the putative Cl^- binding site in βENaC reduced ENaC regulation by Cl^-, but it had no effect on Na^+ self-inhibition (Fig. 5*D*). These observations suggest that in addition to its effect on Na^+ self-inhibition, Cl^- may have a direct effect on ENaC activity that is independent of its effect on Na^+ self-inhibition.

We found that extracellular protons alter the effect of Cl^- on ENaC; acidic pH enhanced inhibition, whereas alkaline pH reduced inhibition. Together with our previous data, this indicates that protons modulate ENaC through at least two independent mechanisms. We propose a model in which titration of the histidine residues that form the Cl^- binding site (His-418 in αENaC and possibly His-396 in γENaC) increase Cl^- binding, resulting in reduced ENaC current at acidic pH. This effect is opposed by titration of additional residues, which decreases Na^+ self-inhibition, resulting in increased current at acidic pH (16). Thus, the net effect of pH on ENaC current is determined by the relative contribution of these two mechanisms. As a result, ENaC regulation by pH might vary under different physiological and pathophysiological conditions. For example, when the Cl^- concentration is low (*e.g.* volume depletion), acidic pH would have a greater stimulatory effect on ENaC than when the Cl^- concentration is high (*e.g.* volume expansion).

ENaC is not the only cation channel that is modulated by extracellular Cl^-. For example, Cl^- and other anions shift the voltage dependence of voltage-gated Na^+ channels (24). The selectivity sequence for voltage-gated Na^+ channels approximated the lyotropic series ($SO_4^{2-} < F^- < Cl^- < NO_3^- < Br^- < I^- < SCN^-$), where the anion effect is primarily related to the energy required for its dehydration rather than the energy of interaction between the anion and its binding site. This situation is observed when the binding site has a relatively low affinity for anions (25). With ENaC, the anion selectivity sequence ($SCN^- < SO_4^{2-} < H_2PO_4^- < F^- < I^- < Cl^- < Br^-$) also corresponded generally to the lyotropic series, although SCN^- and I^- were displaced from their predicted positions. Together with the Cl^- dose-response relationship, the data indicate that the ENaC binding site has a relatively low affinity for anions. This feature is important because it allows ENaC to be regulated by Cl^- concentrations found in urine and airway surface liquid.

What is the physiological role of ENaC regulation by Cl^-? In the kidney collecting duct, the urine Na^+ and Cl^- concentrations can vary over a wide range (19). Previous work indicates that changes in Na^+ concentration regulate the rate of Na^+ transport through two distinct mechanisms: Na^+ self-inhibition (13–15) and Na^+ feedback inhibition (26–31). We speculate that Cl^- regulates Na^+ transport in an analogous manner. For example, a drop in collecting duct Cl^- concentration under conditions of hypovolemia would facilitate Na^+ absorption, whereas increases in Cl^- concentration in hypervolemia would reduce Na^+ absorption. Similar to ENaC regulation by Na^+, this mechanism may function to maintain Na^+ and volume homeostasis. Regulation of ENaC by Cl^- may also serve to indirectly regulate Cl^- absorption because the transport of Cl^- is coupled to Na^+ transport to maintain electroneutrality. Together with previous work, our findings support a model in which the extracellular domains of ENaC function as sensors by which a variety of extracellular signals modulate epithelial Na^+ absorption.

Acknowledgments—We thank Diane Olson, Kaela Kramer, Caitlin Digman, and Zeru Peterson for assistance. We acknowledge the University of Iowa In Vitro Models and Cell Culture Core for providing primary airway cultures and the University of Iowa DNA Core Facility for reagents and DNA sequencing.

REFERENCES

1. Canessa, C. M., Schild, L., Buell, G., Thorens, B., Gautschi, I., Horisberger, J. D., and Rossier, B. C. (1994) *Nature* **367,** 463–467
2. McDonald, F. J., Price, M. P., Snyder, P. M., and Welsh, M. J. (1995) *Am. J. Physiol.* **268,** C1157–1163
3. Schild, L. (2004) *Rev. Physiol. Biochem. Pharmacol.* **151,** 93–107
4. Snyder, P. M. (2005) *Endocrinology* **146,** 5079–5085
5. Lifton, R. P. (1996) *Science* **272,** 676–680
6. Boucher, R. C., Stutts, M. J., Knowles, M. R., Cantley, L., and Gatzy, J. T. (1986) *J. Clin. Invest.* **78,** 1245–1252
7. Jasti, J., Furukawa, H., Gonzales, E. B., and Gouaux, E. (2007) *Nature* **449,** 316–323
8. Lingueglia, E., Champigny, G., Lazdunski, M., and Barbry, P. (1995) *Nature* **378,** 730–733
9. Tavernarakis, N., and Driscoll, M. (1997) *Annu. Rev. Physiol.* **59,** 659–689
10. Vallet, V., Chraibi, A., Gaeggeler, H. P., Horisberger, J. D., and Rossier, B. C. (1997) *Nature* **389,** 607–610
11. Hughey, R. P., Bruns, J. B., Kinlough, C. L., Harkleroad, K. L., Tong, Q., Carattino, M. D., Johnson, J. P., Stockand, J. D., and Kleyman, T. R. (2004) *J. Biol. Chem.* **279,** 18111–18114
12. Caldwell, R. A., Boucher, R. C., and Stutts, M. J. (2004) *Am. J. Physiol. Cell Physiol.* **286,** C190–194
13. Garty, H., and Palmer, L. G. (1997) *Physiol. Rev.* **77,** 359–396
14. Chraïbi, A., and Horisberger, J. D. (2002) *J. Gen. Physiol.* **120,** 133–145
15. Sheng, S., Bruns, J. B., and Kleyman, T. R. (2004) *J. Biol. Chem.* **279,** 9743–9749
16. Collier, D. M., and Snyder, P. M. (2009) *J. Biol. Chem.* **284,** 792–798
17. Sheng, S., Perry, C. J., and Kleyman, T. R. (2002) *J. Biol. Chem.* **277,** 50098–50111
18. Sheng, S., Perry, C. J., and Kleyman, T. R. (2004) *J. Biol. Chem.* **279,** 31687–31696
19. Rose, B. D. (1984) *Clinical Physiology of Acid-Base and Electrolyte Disorders*, pp. 274–275, McGraw-Hill, New York
20. McDonald, F. J., Snyder, P. M., McCray, P. B., Jr., and Welsh, M. J. (1994) *Am. J. Physiol.* **266,** L728–734
21. Karp, P. H., Moninger, T. O., Weber, S. P., Nesselhauf, T. S., Launspach, J. L., Zabner, J., and Welsh, M. J. (2002) *Methods Mol. Biol.* **188,** 115–137
22. Dinudom, A., Young, J. A., and Cook, D. I. (1993) *J. Membr. Biol.* **135,** 289–295
23. Snyder, P. M., Bucher, D. B., and Olson, D. R. (2000) *J. Gen. Physiol.* **116,** 781–790
24. Dani, J. A., Sanchez, J. A., and Hille, B. (1983) *J. Gen. Physiol.* **81,** 255–281
25. Hille, B. (1992) *Ionic channels of Excitable Membranes*, pp. 288–290, Sinauer Associates, Inc., Sunderland, MA
26. Komwatana, P., Dinudom, A., Young, J. A., and Cook, D. I. (1996) *Proc. Natl. Acad. Sci. U.S.A.* **93,** 8107–8111
27. Kellenberger, S., Gautschi, I., Rossier, B. C., and Schild, L. (1998) *J. Clin. Invest.* **101,** 2741–2750
28. Awayda, M. S. (1999) *Am. J. Physiol.* **277,** C216–224
29. Abriel, H., and Horisberger, J. D. (1999) *J. Physiol.* **516,** 31–43
30. Anantharam, A., Tian, Y., and Palmer, L. G. (2006) *J. Physiol.* **574,** 333–347
31. Knight, K. K., Wentzlaff, D. M., and Snyder, P. M. (2008) *J. Biol. Chem.* **283,** 27477–27482